Int J Clin Exp Med 2019;12(6):6604-6616
www.ijcem.com /ISSN:1940-5901/IJCEM0090260

Original Article

Comparative proteomic analysis of acetylation profiles in esophageal squamous carcinoma cells

Yaqing Dai, Qiwei Yao, Weijie Sun, Jiancheng Li

Department of Radiation Oncology, Fujian Medical University Cancer Hospital, Fujian Cancer Hospital, Fuzhou 350014, Fujian, China

Received December 22, 2018; Accepted April 9, 2019; Epub June 15, 2019; Published June 30, 2019

Abstract: Objective: The current study aimed to explore differential expression levels of proteins and acetylation between esophageal squamous carcinoma cells (ESCCs) and cancer stem-like cells (CSCs) using proteomic analysis. Materials and methods: Eca-109 cells were divided into the CSCs group and ESCCs group by serum-free and serum culturing. This study measured CD44 expression, cell proliferation, and plate cloning formation, aiming to identify characteristics of cancer stem cells. Furthermore, Tandem Mass Tags (TMT)-based quantitative proteomics and bioinformatic analysis were used to analyze proteomics. Results: Positive rates of CD44 and proliferation rates in the CSCs group were higher than those in the ESCCs group. Plate cloning formation showed that D0, Dq, N, and SF2 values were significantly higher in the CSCs group, with a radiation sensitization ratio of 1.556. Furthermore, a total of 5,262 proteins and 687 acetylated sites in 433 proteins were identified. In addition, 53 acetylated sites were increased, while 67 acetylated sites were decreased in CSCs group. The most conspicuous regulation in histones of ESCC was histone H3.3 and histone H1x, while the most in acetylated non-histones were histone-lysine N-methyltransferase NSD2 and transmembrane and TPR repeat-containing protein 3. Bioinformatic analysis further revealed that those acetylated sites were involved in DNA metabolism, cell adhesion, glycolysis and gluconeogenic pathways, carbon metabolism, and protein processing in the endoplasmic reticulum. Conclusion: The current study provides a comparative survey of proteins and lysine-acetylation in ESCCs and CSCs. Differentially-expressed proteins and acetylation could be a potential new target for esophageal squamous carcinoma treatment.

Keywords: Proteomics, acetylation, esophageal squamous carcinoma, cancer stem-like cells

Introduction

Worldwide, incidence rates of esophageal cancer rank eleventh for all cancers, while ranking ninth in mortality. Half of the cases of esophageal cancer have occurred in China, with ESCC accounting for approximately 90% of the cases [1-3]. However, 5-year overall survival rates for ESCCs treated with a combination of surgery, radiotherapy, and chemotherapy remain less than 20% [4].

CSCs are a subgroup of tumor cells. They are resistant to many conventional therapies through self-renewal and proliferation [5-9]. It has been shown that CSCs contribute to occurrence, development, recurrence, metastasis, and the failure of conventional cancer therapies [10, 11]. CD44 is a marker for esophageal cancer stem cells, used to screen for esophageal cancer stem cells [12]. Acetylation is involved in various stemness-related signal pathways, influencing their functional roles in sustaining CSCs properties [13]. Moreover, H3 hypoacetylation had been found to correlate with the severity and histological differentiation of ESCC, suggesting that aberrant histone acetylation might play a large role in the development and progression of ESCC [14]. Currently, there are no effective targeted therapy measures for esophageal cancer. Therefore, with the goal of developing new targets for CSCs, investigators are currently studying several proteins and modification sites intended to target CSCs [15-17]. However, there is no comprehensive information on proteins and acetylation in CSCs of ESCC. The most critical issue is that key acetylated proteins and sites between ESCCs and CSCs remain unclear. Studying the acetylation-related biological regulation of

ESCCs and CSCs might provide new insight, leading to better treatment methods for ESCC.

Tandem Mass Tags (TMT)-based quantitative proteomics relies heavily on mass spectrometry, with high sensitivity, high-throughput, and high automation. It has been widely used in drug targeting and disease resistance research [18, 19]. The current study used a combination of TMT labeling and liquid chromatography-tandem mass spectrometry (LC-MS/MS) synthesis to quantify changes in protein acetylation, including histone or non-histone proteins of ESCCs and CSCs. Bioinformatic analysis was further used to analyze quantifiable proteins and acetylation, aiming to reveal the biological characteristics of ESCCs and CSCs, providing new insight for targeted therapy measures for ESCC at the molecular level.

Materials and methods

Cell sphere-forming culture

Human esophageal squamous carcinoma Eca-109 cell lines (ESCCs) were purchased from Shanghai Biological Cell Bank (Shanghai, China). The cells were cultured in serum-supplemented medium (SSM) containing RPMI-1640 medium (Gibco, United States), 10% fetal calf serum (FBS) supplemented with 100 U/mL penicillin, and 100 μg/mL streptomycin. It was incubated at 37°C in a 5% CO_2 humidity incubator. Cells were passaged every 2 days. Cells in the logarithmic phase were chosen for experimentation. The serum free medium (SFM) consisted of RPMI-1640 (1:1), B27 (1:50) (Gibco, United States), epidermal growth factor (20 ng/mL), basic fibroblast growth factor (20 ng/mL), insulin 5 μg/mL, transferrin 10 μg/mL, and 0.5% bovine serum albumin. The cells were resuspended in SFM and plated in low adhesion 6-well culture plates (Corning, United States) at 1×10^5 cells/well. They were then incubated at a constant temperature with a humidity incubator (37°C, 5% CO_2). Fresh SFM (1 mL) was added every other day to replenish the old medium.

Self-renewal and induced differentiation of cell spheres

Logarithmic phase Eca-109 cells were collected. Moreover, 0.25% pancreatin containing 0.02% EDTA was used to digest monolayer adherent cultured Eca-109 cells. The supernatant was discarded after centrifugation and SFM was added for blowing to mix fully into a single cell suspension. The cells were then plated in low adhesion 6-well culture plates at 1×10^5 cells/mL, with 2 mL/well. Every other day, Fresh SFM (1 mL) was added to replenish the old medium. Cell spheres were collected 6-8 days after routine culturing, then mechanically dispersed to form a single cell suspension. Next, after centrifugation and 0.01M PBS washing 1 time, the cells were resuspended in the SFM. They were then incubated at constant temperature with a humidity incubator (37°C, 5% CO_2). After 6 to 8 days of culturing, the cells were passaged at a proportion of 1:2. Cell spheres formed 10 days after culturing in SFM. They were placed in SSM again and differentiated. Morphological changes were observed under an inverted microscope.

Cell proliferation assay

Eca-109 cells and cell spheres (CSs) were, respectively, made into two single cell suspensions. They were placed in 96-well plates at a density of 1×10^4 cells/well in a volume of 100 μL/well. Cell Counting Kit-8 (CCK-8) was used to determine cell proliferation of the two groups for 0, 24, 48, and 72 hours, respectively, with 6 wells per time period. Next, the mixture was added with 100 μl/well of fresh medium, containing 10% CCK-8. After the cells were incubated at 37°C for 2 hours, absorbance values were detected at 450 nm on a microplate reader. A cell growth curve was plotted with A450 on the Y axis and time on the X axis. Growth curves of two group cells are shown for each treatment at 0, 24, 48, and 72 hours.

Colony forming ability and clone formation assay

Adherent culture cells and cell spheres were digested and evenly inoculated into 6-well plates at different densities. They were then subjected to different irradiation doses (0, 2, 4, 6, and 8 Gy). Three samples were used in each group and each irradiation dose. The cells were then cultured for 10-14 days after irradiation. Next, the cells were fixed in methanol and stained with crystal violet. Cell colonies were observed and counted. The size and number of cell colonies were further compared. Cell colonies with more than 50 cells were counted

under microscopy. A medical linear accelerator (Varian, United States) was then employed for radiation, with a 6 MV X-ray, 30 cm×30 cm beam size, and 1 Gy/min dosage rate, as well as a radiation source at a distance of 100 cm from the cell growth surface. Planting efficiency in different experimental conditions was calculated. Planting efficiency: PE (%) = colony number/inoculated cells×100% and survival fraction; SF = colony number in one irradiation dose group/(inoculated cells in the group×PE in the non-irradiation group). A cell survival curve was fitted using a multi-target single-hit model S = 1 - (1-e-D/Do) N using GraphPad Prism 5 Demo software. Radiobiological parameters, D0, Dq, and SF2, were assayed and calculated. Independent experiments were repeated 3 times.

Detection of cell surface markers CD44+

Suspended cultured esophageal cancer cell spheres, passaged after 3 generations, and cultured adherent cancer cells were collected. The cells were digested or mechanically dispersed into single cell suspensions 24 hours after irradiation. Cells at a density of 1×10^5/100 μL were incubated with rat against human CD44-FITC (Abcam, United States). No antibodies were added to the control group. Cells were then incubated for 30 minutes at 4°C in the dark. They were rinsed twice in PBS, followed by detection using flow cytometry. All experiments were carried out in triplicate within 1 hour of staining. All experiments were repeated three times. CD44+ esophageal squamous cell lines were separated from tumor cells using flow separation technology. They were defined as CSCs, while CD44-esophageal squamous cell lines separated from adherent cells were defined as ESCCs.

TMT and proteomic quantification

Next, TMT and mass spectrometry (MS) data acquisition was conducfted. Briefly, CSCs and ESCCs were used to quantify dynamic changes of lysine acetylation through an integrated approach, involving TMT coupled with MS-based quantitative proteomics. First, CSCs and ESCCs cells were labeled with the 4-plex TMT kit. Briefly, one unit of TMT reagent (Thermo, USA) was defined as the amount of reagent required to label 1 mg of protein. The two cell lines exhibited > 97% labeling efficiency. They were harvested and lysed for protein extraction. After digestion with trypsin, the resulting peptides were immuno-precipitated with anti-Kac pan-antibodies (1:200; PTM Biolab, Zhejiang, China) to enrich for acetylated lysine peptides. Finally, the enriched Kac-containing peptides from each cell line were subjected to HPLC-MS/MS analysis. HPLC-MS/MS was performed using an LTQ Orbitrap Velos mass spectrometer (Thermo Scientific, MA, USA), coupled with an Eksigent nanoLC-1D plus pump (Eksigent Technologies, CA, USA). Mass spectra were generated by Fourier Transform mass spectrometry (FTMS) using the Orbitrap™ analyzer at 70,000 resolution and 100 m/z. This was followed by collision-induced dissociation (CID) in the Velos™ dual cell linear trap at 35% normalized collision energy. MS/MS data were processed using MaxQuant integrated with the Andromeda search engine (v.1.5.2.8). Tandem mass spectra were searched against the SwissProt human database (20,130 protein sequences).

Protein-protein interaction analysis

Kac protein identification was searched against the STRING (http://string-db.org/) database version 10.0 for protein-protein interactions. Only interactions between the proteins contained in the searched data set were selected. STRING defines a metric called “confidence score” to define interaction confidence. Interactions are fetched when a confidence score is ≥ 0.7 (high confidence). The interaction network from STRING was visualized using Cytoscape (http://www.cytoscape.org/v.3.2.1).

Statistical analysis

MS/MS data were processed using MaxQuant integrated with the Andromeda search engine (v.1.5.2.8). Tandem mass spectra were searched against the SwissProt human database. Expression changes of more than 1.5-fold were set as the differentially quantified threshold. Data are expressed as the mean ± SD of at least three independent experiments. Proliferation of Eca-109 adherent cells and Eca-109 spheres, as well as clonal formation of adherent cells and CSs, were compared using Student’s t-tests. Optical densities of the Eca-109 adherent cells and Eca-109 spheres for 0, 24, 48, and 72 hours, as well as the SF of the Eca-109 CSs and Eca-109 cells for 0, 2, 4, 6,

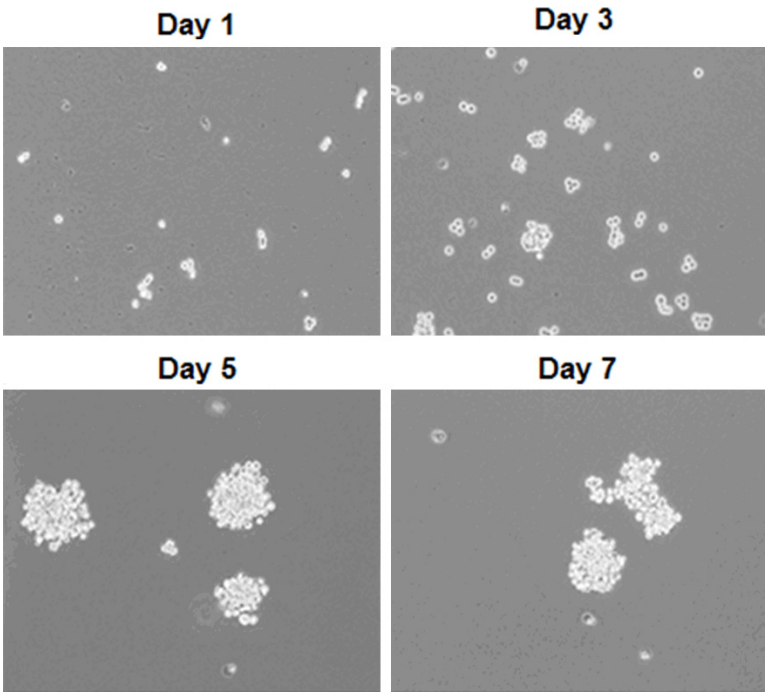

Figure 1. Observation under an inverted phase contrast microscope indicates most cell spheres adhered after 1, 3, 5, and 7 days (×200, 1×10^5 cells/mL).

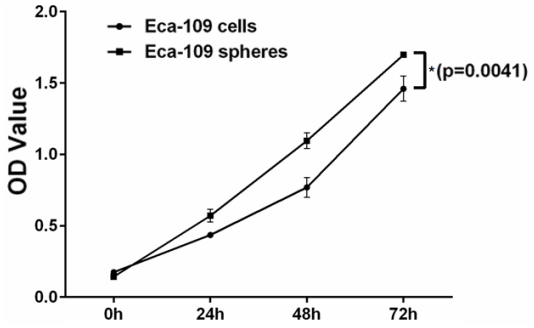

Figure 2. Cell growth was determined by CCK-8 assays. The multiplication capacity of Eca-109 cell spheres was significantly higher than that of normal adherent cells.

and 8 Gy, were analyzed for variance using ANOVA. All analyses used GraphPad Prism 5.0 software. $P < 0.05$ indicates statistical significance.

Results

Culture and multiplication capacity of CSCs

Cell spheres (CSs) have characteristics of CSCs. They were isolated from Eca-109 cells with 1 x 10^5 cell /mL density in a serum-free suspension culture. The cells were visualized with an inverted phase contrast microscope. Cell clusters of different sizes were suspended in SFM. After a time period, the tumor spheres were gradually enlarged and rounded (**Figure 1**). CCK-8 was used to measure optical densities of the two group cells for 0, 24, 48, and 72 hours, respectively. Results showed that the proliferative capacity of tumor spheres was significantly higher than that of adherent cells ($P < 0.05$, **Figure 2** and **Table 1**).

Colony forming ability, colony forming efficiency (CFE), and flow cytometry

The clonal formation ability of adherent cells was compared with that of the CSs. After crystal violet staining, clonal groups visible to the naked eye were photographed and counted. Sizes and numbers of clonal groups were compared, respectively (**Figures 3**, **4**). The ability of clonal formation of adherent cells and CSs was compared. The clonal formation rate of adherent cells was 32.5 ± 4.203%, while that of CSs was 63.75 ± 6.652%, with statistically significant differences ($P < 0.05$, **Figure 3**). After irradiation, the formation rate of CSs increased gradually with doses of 2, 4, and 6 Gy ($P < 0.05$, **Figure 5**). Results showed that irradiation improved the formation rate of CSs in Eca-109 lines *in vitro*. Eca-109 CSs and Eca-109 cells D0 were 3.103 and 1.981. Eca-109 CSs and Eca-109 cells Dq were 3.33 and 0.872. Eca-109 CSs and Eca-109 cells N were 1.553 and 2.927. Eca-109 CSs and Eca-109 cells SF2Gy were 0.507 and 0.890 ($P < 0.05$). Results showed that Eca-109 CSs had stronger radiation resistance than Eca-109 cells. The sensitization ratio was 1.556 (**Figure 6**, **Table 2**). Results also showed that expression of CD44+ in CSs was 66.74%, markedly higher than that in Eca-109 cells (**Figure 7**). CD44+ esophageal squamous cell lines were CSCs, while CD44-esophageal squamous cell lines were ESCCs.

Table 1. Comparison of proliferation of Eca-109 adherent cells and Eca-109 spheres

Group	0	24 h	48 h	72 h
Eca-109 cells cell	0.1751 ± 0.01382	0.4358 ± 0.01831	0.7686 ± 0.06916	1.460 ± 0.08790
Eca-109 spheres	0.1430 ± 0.01744	0.5703 ± 0.04437	1.096 ± 0.05481	1.698 ± 0.01619
P value	0.0271	0.0008	0.0005	0.0041

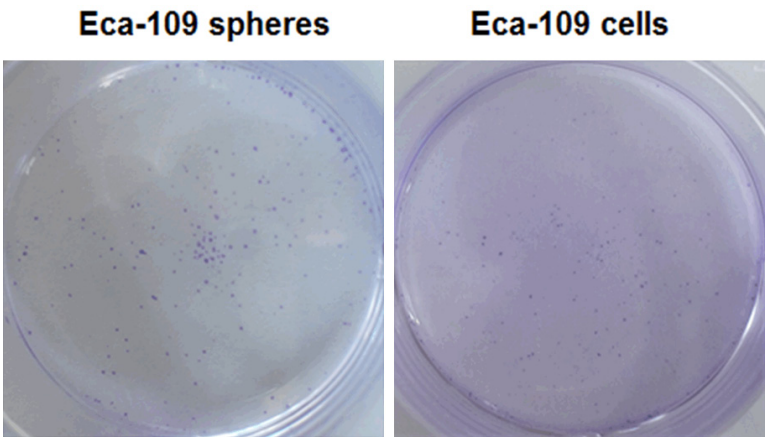

Figure 3. Eca-109 spheres and Eca-109 cells were cultured for 13 to 15 days and stained with crystal violet.

Quantification overview of proteins and acetylated sites

Present results indicated that a total of 5,262 proteins were identified in the two groups. Upregulation of 187 proteins and downregulation of 83 proteins were detected in the CSCs group, compared to the ESCCs group (> 1.5 times). In addition, 53 acetylated sites on 46 proteins were increased, while 67 acetylated sites on 60 proteins were decreased in the CSCs group (> 1.5 times) (**Figure 8**). Scatter diagrams were used to verify that there were no significant differences concerning differential expression levels of acetylated proteins in 2 paired cells (y = 0.8671x-0.7361, R2 = 0.4013).

Protein annotation

For histone acetylation differentially-expressed by CSCs and ESCCs, histone H1x was noted for the largest changes of downregulation. Histone H3.3 showed the greatest degree of upregulation in ESCCs. Additionally, transmembrane and TPR repeat-containing protein 3 was the acetylated non-histone with the most upregulation, while histone-lysine N-methyltransferase NSD2 showed the most downregulation.

Motif analysis of acetylation

In the CSCs, 4 acetylation site motifs (10 amino acids, both upstream and downstream of the acetylation lysine site (Kac)) were identified, based on 682 unique acetylated sites using the Motif-X program. KacK, KacR, Kac.K, and Kac.K, were enriched and conserved. A motifs enrichment heat map (**Figure 9**) showed the abundance or loss of special amino acids adjacent to Kac sites. Lysine (K), Alanine (A), arginine (R), and glycine (G) were significantly increased around Kac sites. The different preferred amino acids surrounding Kac reflected the special recognition of the enzymes that catalyzed acetylation in each group. Further investigation is necessary to explore the activity of different enzymes in these sites.

Functional annotation of the Lys acetylome in ESCC

GO annotation analysis was used to further recognize characteristics of the identified acetylated proteins (**Figure 10**). According to GO annotation, the functions of acetylated proteins were divided into cell component, molecular function, and biological process.

Results of cell component revealed that upregulated and downregulated acetylated proteins were mainly distributed in cells (21% and 22%), organelles (21% and 21%), membrane-enclosed lumen (14% and 15%), extracellular region (14% and 11%), membranes (11% and 12%), and macromolecular complex (11% and 19%). Regarding biological processes, overexpression or low-expression of acetylated proteins in CSCs were involved in the cellular process (15% and 15.3%), metabolic process (11% and 13.0%), single-organism process (13% and 12.3%), and biological regulation (10% and

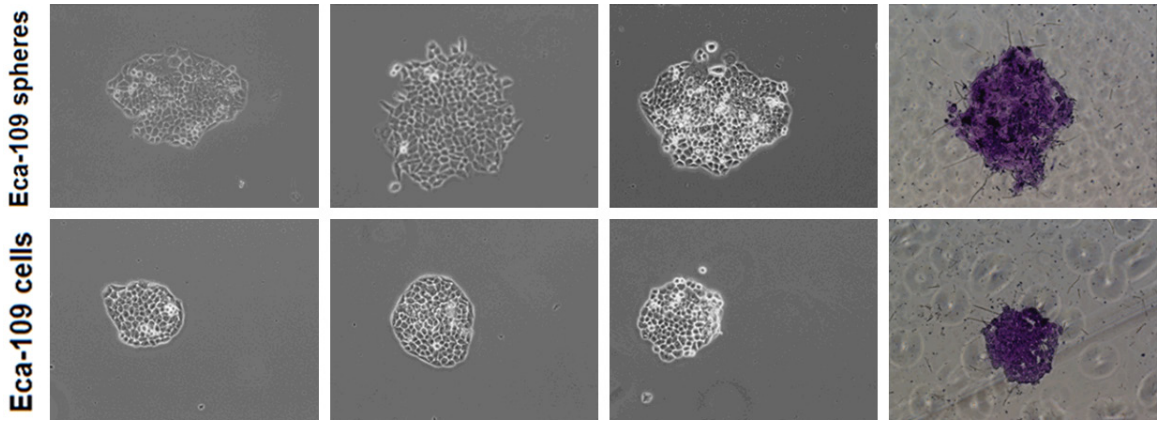

Figure 4. Comparison of sizes of Eca-109 spheres and Eca-109 cells clones.

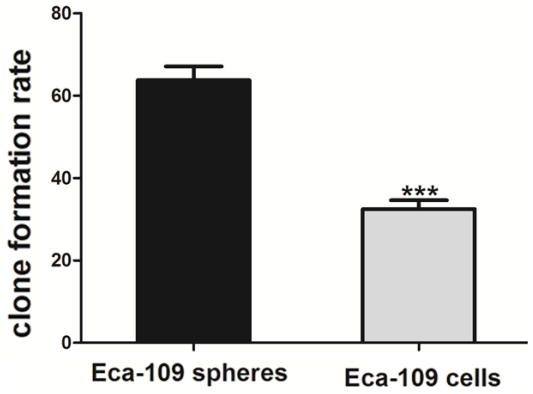

Figure 5. Comparison of clone formation rates between Eca-109 spheres and Eca-109 cells. Error bars represent mean ± SD. ***$P < 0.001$ versus Eca-109 spheres group.

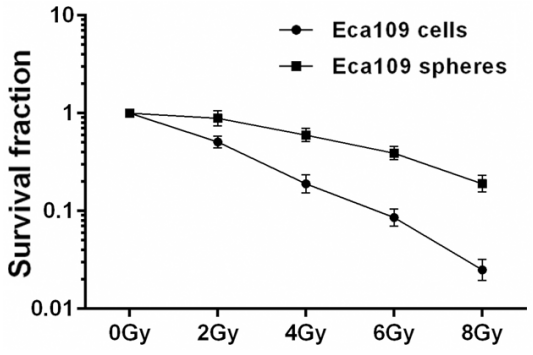

Figure 6. Differences in sensitivity to radiation between cell spheres and adherent cells, compared in a clone formation assay. Cell spheres were also more radioresistant than parent cells ($P < 0.05$).

11%). Based on molecular function classification, under-expressed or over-expressed acetylated proteins mainly associated with binding (51% and 55%) and catalytic activity (29% and 19%). Analysis of subcellular localization elucidated the proteins function. Present data showed that upregulated acetylated proteins were widely localized in the cytoplasm (44%), mitochondria (24%) and nucleus (22%). However, downregulated acetylated proteins were found in the nucleus (43%), cytoplasm (25%), and mitochondria (10%) (**Figure 10**).

Enrichment and clustering analysis of acetylation data sets

To further elucidate cellular functions involving acetylation in ESCC, acetylated proteins were divided into three categories, including biological process, cell component, and molecular function, by GO annotation.

In the cellular component category, the upregulated protein cluster was mainly distributed in the extracellular component (exosome, vesicle, organelle), supramolecular component (fiber, complex, polymer), and chaperone complex (chaperonin-containing T-complex). The downregulated protein cluster was distributed in cell-substrate adherens junction, nucleolus, and complex (SWI/SNF, BAF-type, nBAF). In agreement with the observation above, evaluation of biological processes showed that acetylated proteins were significantly involved in DNA metabolic processes and chaperone-mediated protein folding in the upregulated proteins. Response to virus, other organisms, external biotic stimulus and biotic stimulus, and multi-organism cellular process were involved in the downregulated ones. Furthermore, molecular function analysis revealed that proteins related

Table 2. Differences in radiobiological parameters between Eca-109 cell spheres and adherent cells compared in a clone formation assay

Groups	D0	Dq	N	SF2	SER
Eca-109 cells	1.981	0.872	1.553	0.507	1.566
Eca-109 spheres	3.103	3.33	2.927	0.890	

to mRNA binding, oxidoreductase activity, pyruvate dehydrogenase (acetyl-transferring), DNA-(apurinic or apyrimidinic site) lyase activity, and activity (protein serine, threonine kinase inhibitor, protein kinase C inhibitor) were enriched in over-expression protein clusters (**Figure 11**).

To further understand cellular pathways involving acetylation in ESCC, KEGG pathways were evaluated. Results showed that upstream signaling pathways in ESCC were mainly associated with biosynthesis of amino acids [-log10 (*p* value) 1.85], pentose phosphate pathway, phagosome [-log10 (*p* value) 1.82], metabolic pathways [-log10 (*p* value) 1.41], PPAR signaling pathways [-log10 (*p* value) 1.38], carbon metabolism [-log10 (*p* value) 1.36], and HIF-1 signaling pathways [-log10 (*p* value) 1.31], while downstream signaling pathways were central to carbon metabolism in cancer [-log10 (*p* value) 1.82], spliceosome [-log10 (*p* value) 1.82], MAPK [-log10 (*p* value) 1.56] and glucagon [-log10 (*p* value) 1.36] signaling pathways (**Figure 12**).

Protein function is largely dependent on specific domain structures in the sequence. To assess the domain structures most regulated in ESCC, domain enrichment analysis was conducted. Protein domains involved in the GroEL-like apical domain were enriched with increased acetylation in CSCs, while the Winged helix-turn-helix DNA-binding domain was enriched mostly in decreased proteins (**Figure 13**).

Protein interaction networks of Lys acetylation proteome

The current study visualized protein-protein interaction networks of 433 Lys acetylated proteins based on the STRING database. A complete network of acetylated proteins was created. The current data set offers an insight into the probability of interactions of acetylated proteins in ESCC. Using the MCODE tool [20], this study identified some highly connected sub-networks among Lys-acetylated proteins, including carbon metabolism and protein processing in the endoplasmic reticulum. The first protein networks were localized to mitochondria, while the others were mainly cytosolic (**Figure 14**).

Discussion

CSCs are the causes of tumorigenesis, invasion, metastasis, and treatment failure. They have strong proliferative capacities, self-renewal abilities, and some special CD markers [10, 21, 22]. Studies have shown that the expression rate of CD44 in esophageal cancer stem cells was much higher than that of parental cells [12]. In this study, tumor spheres obtained from the serum-free suspension culture were taken to clarify that esophageal cancer stem cells have strong proliferation ability and colony forming ability. They were then shown to have certain radio-resistance, according to colony formation tests. Finally, CD44-positive tumor cells were screened by flow cytometry as ECSCs.

Lysine acetylation plays an important role in chromatin structure and transcription regulation [20, 23]. Acetylation is involved in various signaling pathways of stem cells, as well as regulated self-renewal and differentiation in normal development. Acetylation further influences cell proliferation, differentiation, and migration by regulating gene expression. Through the above regulating mechanisms, acetylation maintains the “stemness” of CSCs and affects occurrence of tumors [24]. Moreover, many studies have confirmed that protein acetylation can be used as a therapeutic target or biomarker for cancer [16, 20, 25]. TMT technology is a relatively new technology of proteomics, based on stable isotope labeling peptides *in vitro* marker technology and tandem mass spectrometry analysis [18, 19, 26].

The current study used TMT and LC-MS/MS analysis of quantitative acetylated proteomics, achieving the profile of protein expression spectrum and acetylated modification spectrum analysis in ESCCs and CSCs. A total of 5,262 proteins were identified. Upregulation of 187 proteins and downregulation of 83 proteins was detected in the CSCs group (> 1.5 times). In addition, 687 acetylated sites in 433 proteins were quantificationally identified in ESCCs in total. Moreover, 53 acetylated sites in 46 proteins were increased, while 67 acetylated sites in 60 proteins were decreased in the

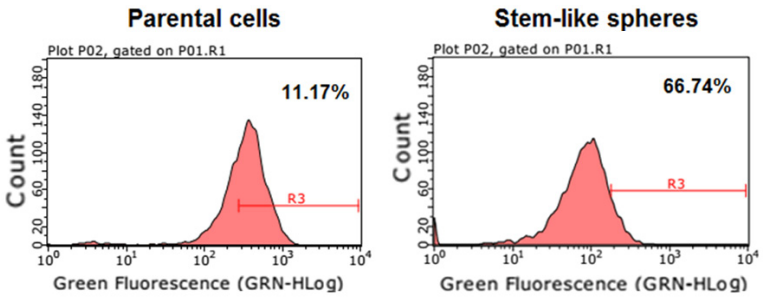

Figure 7. Proportion changes of CD44+ cells in parental cells and stem-like spheres with different doses of radiation. Expression of CD44+ cells was detected using flow cytometry.

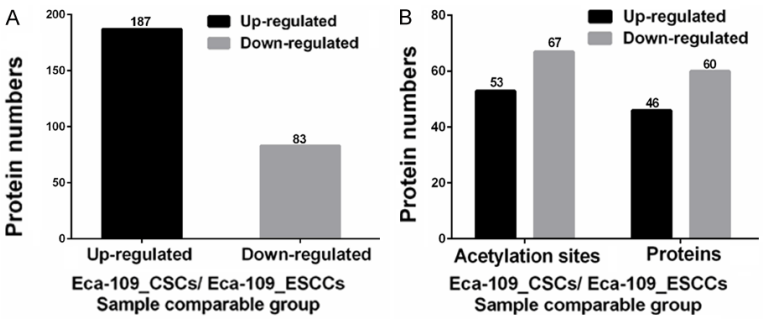

Figure 8. A. Different expression levels in proteins; B. Different expression levels in acetylation sites.

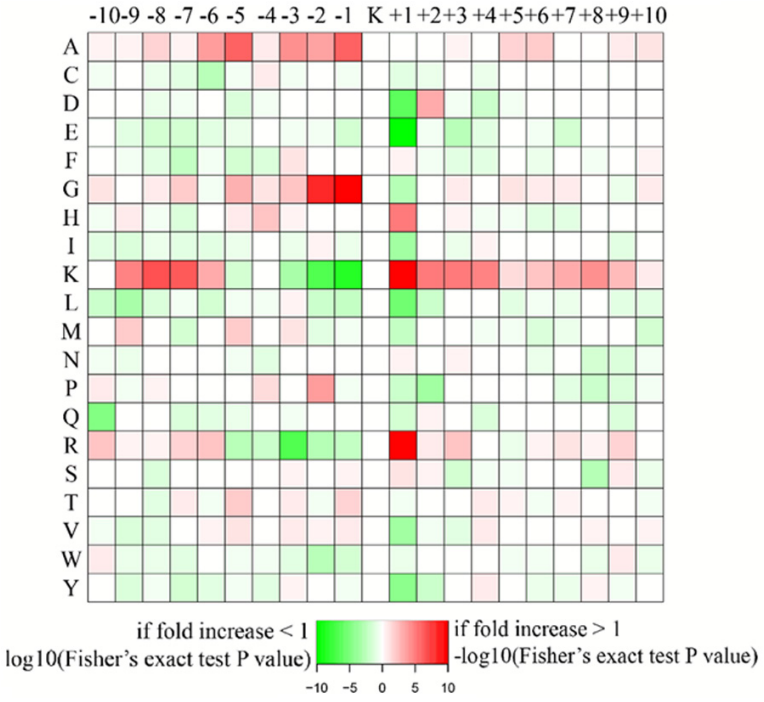

Figure 9. Heat maps showing the frequency of the amino acids present surrounding acetylated sites. The colors represent enrichment (red) or depletion (green) of amino acids at the specific positions.

CSCs group (> 1.5 times). This study revealed a worldwide view of proteins and acetylation involved in ESCCs for the first time.

To further study the properties of quantitatively identified acetylated proteins, GO annotation was used to analyze and exploit biological functions of the acetylation. Results showed that acetylation of the ESCC was mainly distributed in cells, organelles, and membrane-enclosed lumen and membranes. They were mainly involved in cellular process, single-organism processes, and metabolic processes. They mainly functioned in the molecular binding and catalytic activity. In addition, through KEGG pathway analysis, this study found that the biosynthesis of amino acids, pentose phosphate pathways, and central carbon metabolism in cancer are among the most famous pathways of CSCs. Carbon metabolism and protein processing in the endoplasmic reticulum were found in the protein-interaction networks. They may be crucial in influencing characteristics of CSCs. The general case of acetylation may greatly promote new cognition of the roles of acetylation in ESCC CSCs.

Histone acetylation uniquely inhibited RNA synthesis, mediated on gene expression and coupled to cellular metabolism [27, 28]. Previous studies have found that hypoacetylation of H3 was related to tumor staging and histological differentiation in ESCC tissues, indicating that this epigenetic phenomenon was related to the invasive nature of

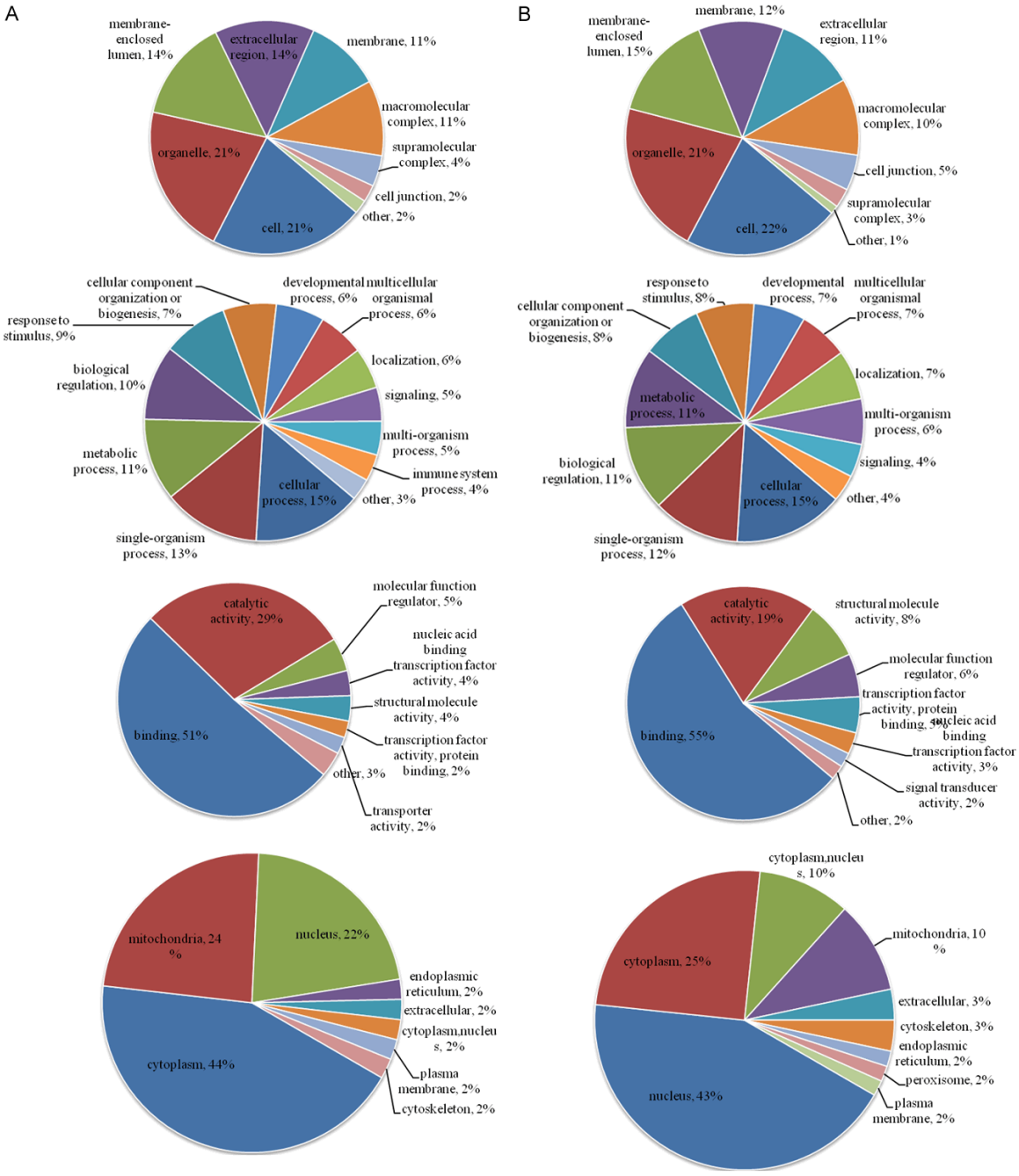

Figure 10. Classification of acetylated proteins based on GO (cellular component, biological process, and molecular function) and subcellular location. (A) Classification of upregulated acetylated proteins in CSCs; (B) Classification of downregulated acetylated proteins in CSCs.

ESCC. Hypoacetylation of histone H4 is more common in patients with a history of drinking. Results indicated that changes in the protein-modifying patterns of the study group might have potential application in the diagnosis and prognosis evaluation of ESCC [14, 29]. Functional studies have shown that p300/CBP-associated factor (PCAF) can inhibit ESCC cell tumorigenicity in formation of lesions and the formation of tumors in nude mice [30]. Concerning acetylated histone proteins expressed in ESCC CSCs, histone H1x was noted for the largest changes of downregulation, while histone-lysine histone H3.3 showed the greatest degree of upregulation in CSCs.

In addition to histone acetylation, biological functions of lysine-acetylation have also made

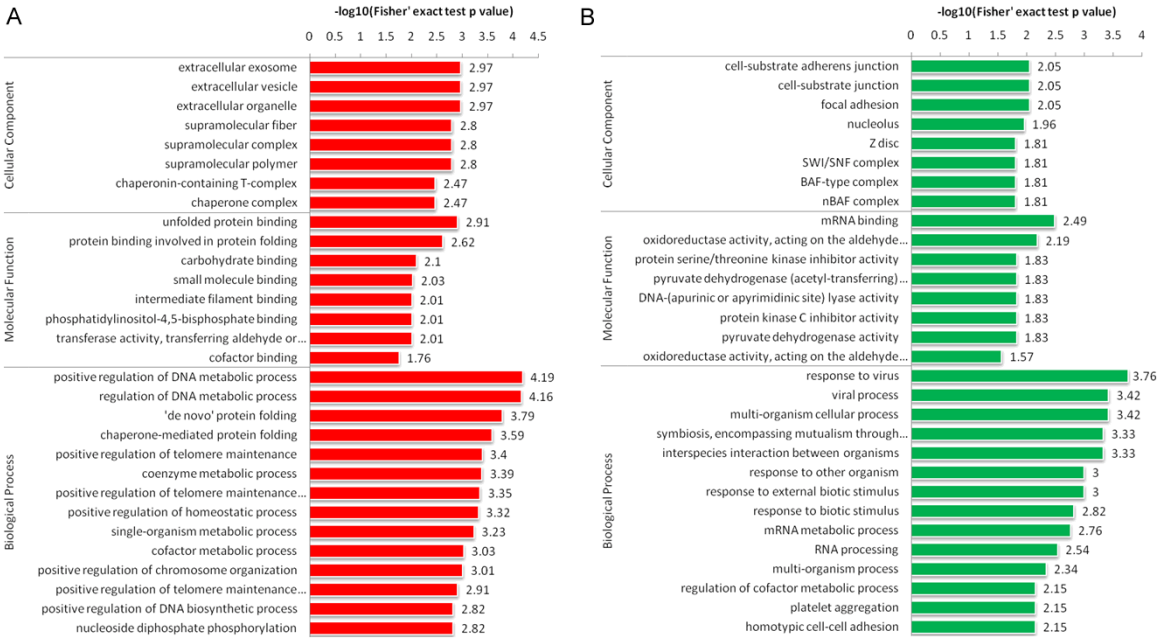

Figure 11. Differentially-expressed lysine acetylated proteins between Eca-109 CSCs and Eca-109 cells were classified by GO annotation based on the following three categories: cellular component, molecular function, and biological process. (A) Enrichment of upregulated acetylated proteins in CSCs; (B) Enrichment of downregulated acetylated proteins in CSCs.

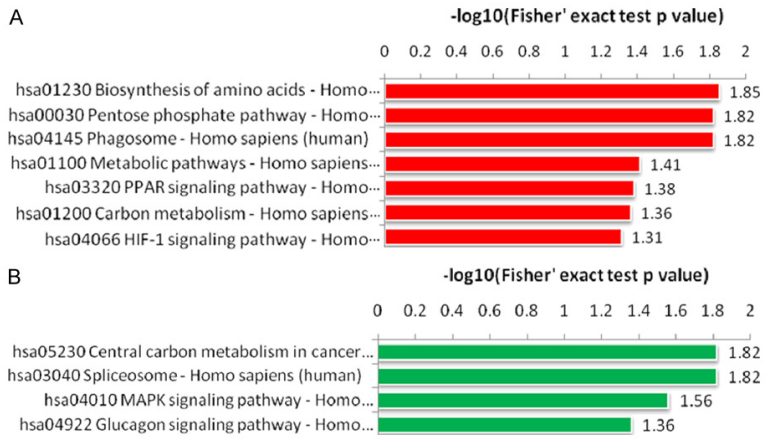

Figure 12. Differentially-expressed lysine acetylated proteins between Eca-109 CSCs and Eca-109 cells were annotated based on the KEGG pathway database. (A) Enrichment of upregulated acetylated proteins in CSCs; (B) Enrichment of downregulated acetylated proteins in CSCs.

progress in non-histones, including many aspects [31-33]. Previous studies have found that acetylation is involved in the endoplasmic reticulum, as a folding control mechanism [34]. Lys acetylation affects the mitochondria and metabolism. A lot of mitochondrial proteins of acetylation could regulate metabolism [35]. Some studies also found that acetylation of p53 impacts DNA-binding affinity and interactions with other proteins [36, 37]. Recently, non-histone proteins targeted by acetylation have been thought to be relevant for human cancers, such as tumorigenesis, cancer cell proliferation, and immune function. In 2015, it was reported that KAT2B acetylation of EZH2 increases the invasive potential of these cancer cells in H1299 cells (NSCLC) [38]. Another study uncovered that amplified in breast cancer1 (AIB1) acetylated by MOF enhanced its function in accelerating breast cancer cell proliferation [39]. Thus far, there have been no reports concerning what and how non-histone acetylation influences ESCCs and CSCs of ESCC, respectively. The current study first showed all acetylated non-histones at different expression levels between CSCs and ESCCs. The greatest increased protein was transmembrane and TPR repeat-containing protein 3. In contrast, the most obvious decreased protein was N-methyltransferase NSD2. These two

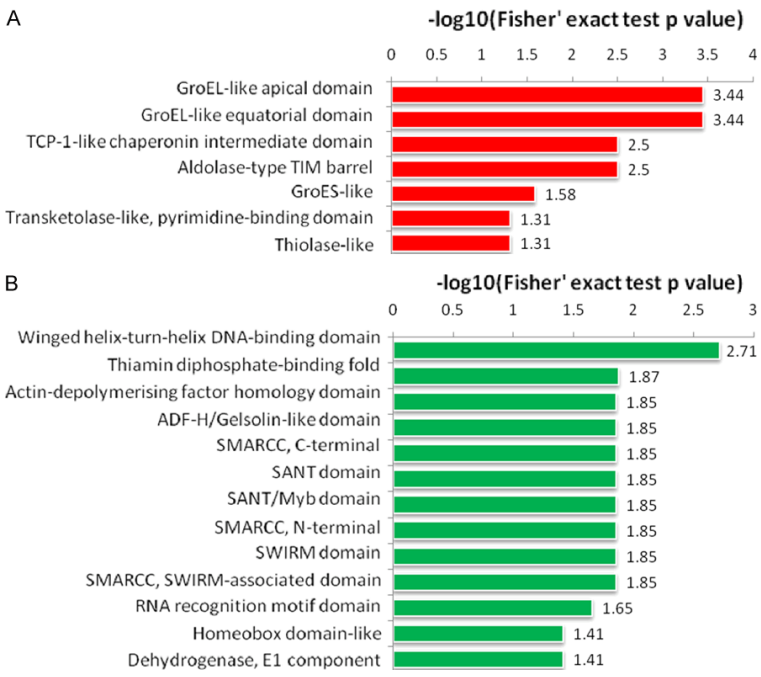

Figure 13. Differentially-expressed lysine acetylated proteins between Eca-109 CSCs and Eca-109 cells were annotated based on the domain structures database. (A) Domain enrichment of upregulated acetylated proteins in CSCs; (B) Domain enrichment of downregulated acetylated proteins in CSCs.

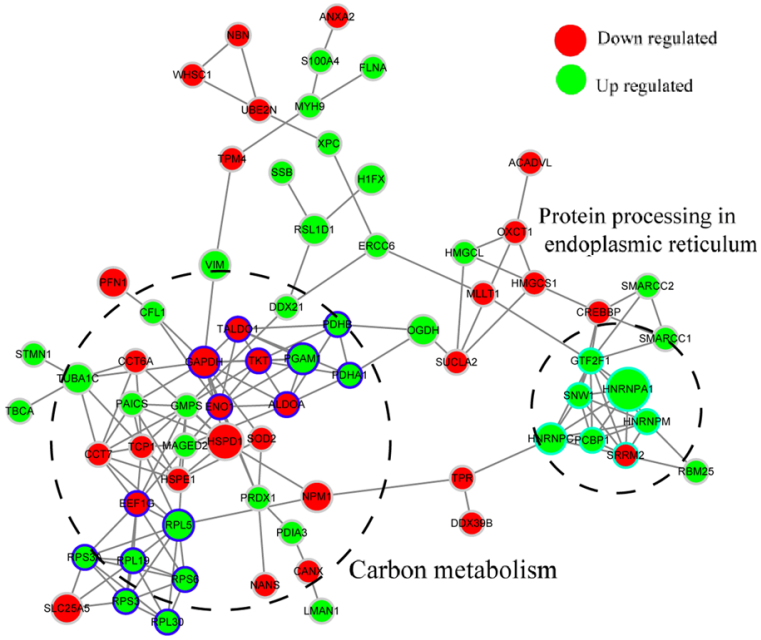

Figure 14. Representative protein-protein interaction network of Lys acetylation proteomes. Interaction networks were analyzed based on the STRING database. Some highly connected subnetworks among Lys-acetylated proteins were identified using the MCODE tool.

most prominent non-histone acetylation factors may be pivotal regulators in CSCs of ESCC.

Conclusion

In summary, current results provide new insight about ESCC, revealing many biological features and differences between CSCs and ESCCs, based on whole-cell proteome and acetylome analyses. A total of 5,262 proteins and 687 acetylated sites in 433 proteins were quantificationally identified in ESCC. The 53 acetylated sites were increased, while 67 acetylated sites were decreased in CSCs and paired ECSSs. This study comprehensively revealed the atlas of proteins and acetylation in ESCC. Furthermore, comparing differentially-acetylated proteins in CSCs and ESCCs, the most unique upregulated in histone of ESCC is histone H3.3. The most downregulated one is histone H1x. Additionally, Histone-lysine N-methyltransferase NSD2 and transmembrane and TPR repeat-containing protein 3 were acetylated non-histones showing the most obvious changes. Differentially-expressed proteins and acetylation factors of CSCs may be related to radio-sensitivity, recurrence, and metastatis of ESCC. Therefore, they could be potential new treatment targets or biomarkers.

Acknowledgements

This work was supported by the Innovation Project of Fujian Provincial Department of Health (2016-CX-10).

Disclosure of conflict of interest

None.

Address correspondence to: Jiancheng Li, Department of Radiation Oncology, Fujian Medical University Cancer Hospital, Fujian Cancer Hospital, No.420, Fuma

Road, Jin'an District, Fuzhou 350014, Fujian, China. Tel: +86-591-83660063; Fax: +86-591-83928767; E-mail: docjianchengli@sina.com

References

[1] Global Burden of Disease Cancer Collaboration, Fitzmaurice C, Dicker D, Pain A, Hamavid H, Moradi-Lakeh M, MacIntyre MF, Allen C, Hansen G, Woodbrook R, Wolfe C, Hamadeh RR, Moore A, Werdecker A, Gessner BD, Te Ao B, McMahon B, Karimkhani C, Yu C, Cooke GS, Schwebel DC, Carpenter DO, Pereira DM, Nash D, Kazi DS, De Leo D, Plass D, Ukwaja KN, Thurston GD, Yun Jin K, Simard EP, Mills E, Park EK, Catalá-López F, deVeber G, Gotay C, Khan G, Hosgood HD 3rd, Santos IS, Leasher JL, Singh J, Leigh J, Jonas JB, Sanabria J, Beardsley J, Jacobsen KH, Takahashi K, Franklin RC, Ronfani L, Montico M, Naldi L, Tonelli M, Geleijnse J, Petzold M, Shrime MG, Younis M, Yonemoto N, Breitborde N, Yip P, Pourmalek F, Lotufo PA, Esteghamati A, Hankey GJ, Ali R, Lunevicius R, Malekzadeh R, Dellavalle R, Weintraub R, Lucas R, Hay R, Rojas-Rueda D, Westerman R, Sepanlou SG, Nolte S, Patten S, Weichenthal S, Abera SF, Fereshtehnejad SM, Shiue I, Driscoll T, Vasankari T, Alsharif U, Rahimi-Movaghar V, Vlassov VV, Marcenes WS, Mekonnen W, Melaku YA, Yano Y, Artaman A, Campos I, MacLachlan J, Mueller U, Kim D, Trillini M, Eshrati B, Williams HC, Shibuya K, Dandona R, Murthy K, Cowie B, Amare AT, Antonio CA, Castañeda-Orjuela C, van Gool CH, Violante F, Oh IH, Deribe K, Soreide K, Knibbs L, Kereselidze M, Green M, Cardenas R, Roy N, Tillmann T, Li Y, Krueger H, Monasta L, Dey S, Sheikhbahaei S, Hafezi-Nejad N, Kumar GA, Sreeramareddy CT, Dandona L, Wang H, Vollset SE, Mokdad A, Salomon JA, Lozano R, Vos T, Forouzanfar M, Lopez A, Murray C, Naghavi M. The global burden of cancer 2013. JAMA Oncol 2015; 1: 505-27.

[2] O'Neill L, Gannon J, Guinan E, Reynolds JV and Hussey J. Multidisciplinary rehabilitation across the esophageal cancer journey. J Thorac Dis 2017; 9: E1140-E1142.

[3] Deng JY, Chen H, Zhou DZ, Zhang JH, Chen Y, Liu Q, Ai DS, Zhu HT, Chu L, Ren WJ, Zhang XF, Xia Y, Sun MH, Zhang HW, Li J, Peng XX, Li L, Han L, Lin H, Cai XJ, Xiang JQ, Chen SF, Sun YH, Zhang YW, Zhang J, Chen HQ, Zhang SJ, Zhao Y, Liu Y, Liang H and Zhao KL. Comparative genomic analysis of esophageal squamous cell carcinoma between Asian and Caucasian patient populations. Nat Commun 2017; 8: 1533.

[4] Chen W, Zheng R, Zhang S, Zeng H, Xia C, Zuo T, Yang Z, Zou X and He J. Cancer incidence and mortality in China, 2013. Cancer Lett 2017; 401: 63-71.

[5] Xie XJ, Teknos TN and Pan QT. Are all cancer stem cells created equal? Stem Cells Translational Medicine 2014; 3: 1111-1115.

[6] Zhou BB, Zhang H, Damelin M, Geles KG, Grindley JC, Dirks PB. Tumour-initiating cells: challenges and opportunities for anticancer drug discovery. Nat Rev Drug Discov 2009; 8: 806-23.

[7] Frank NY, Schatton T and Frank MH. The therapeutic promise of the cancer stem cell concept. J Clin Invest 2010; 120: 41-50.

[8] Ho MM, Ng AV, Lam S and Hung JY. Side population in human lung cancer cell lines and tumors is enriched with stem-like cancer cells. Cancer Res 2007; 67: 4827-4833.

[9] Hu XQ, Cong Y, Luo H, Wu SJ, Zhao L, Liu QT and Yang YL. Cancer stem cells therapeutic target database: the first comprehensive database for therapeutic targets of cancer stem cells. Stem Cells Transl Med. 2017; 6: 331-334.

[10] Lopez-Gomez M, Casado E, Munoz M, Alcala S, Moreno-Rubio J, D'Errico G, Jimenez-Gordo AM, Salinas S and Sainz B Jr. Current evidence for cancer stem cells in gastrointestinal tumors and future research perspectives. Crit Rev Oncol Hematol 2016; 107: 54-71.

[11] Eun K, Ham SW and Kim H. Cancer stem cell heterogeneity: origin and new perspectives on CSC targeting. BMB Rep 2017; 50: 117-125.

[12] Li JC, Liu D, Yang Y, Wang XY, Pan DL, Qiu ZD, Su Y and Pan JJ. Growth, clonability, and radiation resistance of esophageal carcinoma-derived stem-like cells. Asian Pac J Cancer Prev 2013; 14: 4891-4896.

[13] Liu N, Li S, Wu N and Cho KS. Acetylation and deacetylation in cancer stem-like cells. Oncotarget 2017; 8: 89315-89325.

[14] Chen C, Zhao M, Yin N, He B, Wang B, Yuan Y, Yu F, Hu J, Yin B and Lu Q. Abnormal histone acetylation and methylation levels in esophageal squamous cell carcinomas. Cancer Invest 2011; 29: 548-556.

[15] Barneda-Zahonero B and Parra M. Histone deacetylases and cancer. Mol Oncol 2012; 6: 579-589.

[16] Wang N, Song X, Liu L, Niu L, Wang X, Song X and Xie L. Circulating exosomes contain protein biomarkers of metastatic non-small-cell lung cancer. Cancer Sci 2018; 109: 1701-1709.

[17] Shen Z, Wang B, Luo J, Jiang K, Zhang H, Mustonen H, Puolakkainen P, Zhu J, Ye Y and Wang S. Global-scale profiling of differential expressed lysine acetylated proteins in colorectal cancer tumors and paired liver metastases. J Proteomics 2016; 142: 24-32.

[18] Moulder R, Bhosale SD, Goodlett DR and Lahesmaa R. Analysis of the plasma proteome using iTRAQ and TMT-based Isobaric labeling. Mass Spectrom Rev 2018; 37: 583-606.

[19] Zhang K, Tang C, Liang X, Zhao Q and Zhang J. Isobaric tags for relative and absolute quan tification (iTRAQ)-based untargeted quantitative proteomic approach to identify change of the plasma proteins by salbutamol abuse in beef cattle. J Agric Food Chem 2018; 66: 378-386.
[20] Karczmarski J, Rubel T, Paziewska A, Mikula M, Bujko M, Kober P, Dadlez M, Ostrowski J. Histone H3 lysine 27 acetylation is altered in colon cancer. Clin Proteomics 2014; 11: 24.
[21] Bai X, Ni J, Beretov J, Graham P and Li Y. Cancer stem cell in breast cancer therapeutic resistance. Cancer Treat Rev 2018; 69: 152-163.
[22] Naderi-Meshkin H, Ahmadiankia N. Cancer metastasis versus stem cell homing: role of platelets. J Cell Physiol 2018; 233: 9167-9178.
[23] Wellen KE, Hatzivassiliou G, Sachdeva UM, Bui TV, Cross JR and Thompson CB. ATP-citrate lyase links cellular metabolism to histone acetylation. Science 2009; 324: 1076-1080.
[24] Zhang E, Han L, Yin D, He X, Hong L, Si X, Qiu M, Xu T, De W, Xu L, Shu Y and Chen J. H3K27 acetylation activated-long non-coding RNA CCAT1 affects cell proliferation and migration by regulating SPRY4 and HOXB13 expression in esophageal squamous cell carcinoma. Nucleic Acids Res 2017; 45: 3086-3101.
[25] Van Damme M, Crompot E, Meuleman N, Mineur P, Bron D, Lagneaux L and Stamatopoulos B. HDAC isoenzyme expression is deregulated in chronic lymphocytic leukemia B-cells and has a complex prognostic significance. Epigenetics 2012; 7: 1403-12.
[26] Rauniyar N and Yates JR 3rd. Isobaric labeling-based relative quantification in shotgun proteomics. J Proteome Res 2014; 13: 5293-5309.
[27] Peleg S, Feller C, Ladurner AG and Imhof A. The metabolic impact on histone acetylation and transcription in ageing. Trends Biochem Sci 2016; 41: 700-711.
[28] Verdin E and Ott M. 50 years of protein acetylation: from gene regulation to epigenetics, metabolism and beyond. Nat Rev Mol Cell Biol 2015; 16: 258-264.
[29] Di Martile M, Del Bufalo D and Trisciuoglio D. The multifaceted role of lysine acetylation in cancer: prognostic biomarker and therapeutic target. Oncotarget 2016; 7: 55789-55810.
[30] Zhu C, Qin YR, Xie D, Chua DT, Fung JM, Chen L, Fu L, Hu L, Guan XY. Characterization of tumor suppressive function of P300/CBP-associated factor at frequently deleted region 3p24 in esophageal squamous cell carcinoma. Oncogene 2009; 28: 2821-2828.
[31] Batta K, Das C, Gadad S, Shandilya J and Kundu TK. Reversible acetylation of non histone proteins: role in cellular function and disease. Subcell Biochem 2007; 41: 193-212.
[32] Glozak MA, Sengupta N, Zhang X and Seto E. Acetylation and deacetylation of non-histone proteins. Gene 2005; 363: 15-23.
[33] Spange S, Wagner T, Heinzel T and Kramer OH. Acetylation of non-histone proteins modulates cellular signalling at multiple levels. Int J Biochem Cell Biol 2009; 41: 185-198.
[34] Costantini C, Ko MH, Jonas MC and Puglielli L. A reversible form of lysine acetylation in the ER and Golgi lumen controls the molecular stabilization of BACE1. Biochem J 2007; 407: 383-395.
[35] Kim SC, Sprung R, Chen Y, Xu Y, Ball H, Pei J, Cheng T, Kho Y, Xiao H, Xiao L, Grishin NV, White M, Yang XJ and Zhao Y. Substrate and functional diversity of lysine acetylation revealed by a proteomics survey. Mol Cell 2006; 23: 607-618.
[36] Brooks CL and Gu W. The impact of acetylation and deacetylation on the p53 pathway. Protein Cell 2011; 2: 456-462.
[37] Reed SM and Quelle DE. p53 acetylation: regulation and consequences. Cancers (Basel) 2014; 7: 30-69.
[38] Wan J, Zhan J, Li S, Ma J, Xu W, Liu C, Xue X, Xie Y, Fang W, Chin YE and Zhang H. PCAF-primed EZH2 acetylation regulates its stability and promotes lung adenocarcinoma progression. Nucleic Acids Res 2015; 43: 3591-3604.
[39] You D, Zhao H, Wang Y, Jiao Y, Lu M and Yan S. Acetylation enhances the promoting role of AIB1 in breast cancer cell proliferation. Mol Cells 2016; 39: 663-668.